Differentiating phase shift and delay in narrow band coherent signals

Muthuraman Muthuraman, Rathinaswamy B. Govindan, Günther Deuschl, U. Heute, Jan Raethjen

Angaben zur Veröffentlichung / Publication details:

Muthuraman, Muthuraman, Rathinaswamy B. Govindan, Günther Deuschl, U. Heute, and Jan Raethjen. 2008. "Differentiating phase shift and delay in narrow band coherent signals." *Clinical Neurophysiology* 119 (5): 1062–70. https://doi.org/10.1016/j.clinph.2008.01.003.

Differentiating phase shift and delay in narrow band coherent signals

M. Muthuraman [a,b], R.B. Govindan [b,c], G. Deuschl [b], U. Heute [a], J. Raethjen [b,*]

[a] *Institute for Circuit and System Theory, Faculty of Engineering, University of Kiel, Kaiserstrasse 2, D-24143 Kiel, Germany*
[b] *Department of Neurology, University of Kiel, Schittenhelmstrasse 10, 24105 Kiel, Germany*
[c] *Department of Obstetrics and Gynecology, University of Arkansas for Medical Sciences, Little Rock, AR 72205, USA*

1. Introduction

In simultaneous recordings of two or more coupled signals from the nervous system we are typically interested in the timing between these activities. In continuous oscillatory activity detecting this timing relationship is not straightforward. Even in cases in which a typical order of activation can be observed in the time domain (e.g. in repetitive burst activity in different muscles) the interpretation of this observation is difficult. Either the order of activation could occur in a fixed pattern as determined by a central generator, or it could be due to a conduction delay, when the activity is transmitted via a defined neuronal pathway. In central pattern generation e.g. in gait (Grillner, 1981, 2006) or rhythmic hand/finger movements (Kay et al., 1991) the activation sequence is fixed whereas the absolute timing may vary with the frequency of the coupled activities. In mathematical terms there is a constant phase shift between the signals with variable time shifts. Conversely, in case of a conduction delay e.g. in corticomuscular (EEG–EMG) coupling (Brown, 2000) the absolute time shift between the coupled signals is determined by the pathway in which the activity is transmitted and is thus relatively fixed, whereas the phase shift is dependent on the coupled frequency. This crucial difference in the frequency dependence of the phase shift can be utilized to distinguish the two if the coupled frequency band is broad enough. The phase shift as calculated and displayed in the phase spectrum will increase or decrease with increasing frequencies when there is a time delay

* Corresponding author. Tel.: +49 (0) 431 597 8515; fax: +49 (0) 431 597 8502.
E-mail address: j.raethjen@neurologie.uni-kiel.de (J. Raethjen).

(Lindemann et al., 2001; Muller et al., 2003) whereas it will remain constant in case of a fixed activation pattern. And even a combination of a fixed pattern and a delay can be determined from the phase spectrum and has been demonstrated for corticomuscular (EEG–EMG) coupling (constant phase shift plus delay (Mima and Hallett, 1999)). However, as the phase can only be interpreted at frequencies at which there is a significant coupling (coherence) between the signals this method fails in case of very narrow-band signals. With such signals there are often only one or two points in the spectrum with a significant coherence (coupling) and thus the frequency dependence of the phase shift cannot be analysed reliably (Hellwig et al., 2000). One typical example of such a narrow-band signal is the tremor in Parkinson's disease (Deuschl et al., 2000). On the basis of MEG and EEG studies (Hellwig et al., 2000; Timmermann et al., 2003; Volkmann et al., 1996) it has been well established that this tremor has a cortical correlate likely contributing to the peripheral tremor by transmission via corticospinal pathways. On the other hand there is a typical pattern of antagonistic muscle activation. It can switch between reciprocal alternating activity and cocontraction but remains relatively fixed over longer periods of time (Spieker et al., 1995; Boose et al., 1996). Thus there is a combination of a relatively fixed pattern between antagonistic muscles in the periphery and a time delay between EEG and these muscles, complicating the estimation of the nature of interaction within this oscillating system. In the present study we apply a new method for delay estimation in narrow band coherent signals (Govindan et al., 2005, 2006) in combination with conventional coherence and phase spectra to a narrow band model system first and then to EEG and EMG data recorded from patients with Parkinsonian tremor. We will show that this combination of mathematical methods allow us to safely distinguish between constant phase shift and delay components within a biological narrow band oscillating system.

2. Methods

2.1. Data acquisition

Eleven recordings from 5 patients (two high-quality recordings in each of 4 patients and three high-quality recordings in 1 patient) with definite Parkinson's disease as diagnosed by the brain bank criteria (Hughes et al., 1992) suffering from a classical Parkinsonian rest tremor (type I) (Deuschl et al., 1998) were included in the study. Four of the patients were male and one female, ages range from 60 to 71 years, with disease durations between 3 and 18 years. In three of them the right side was more affected in the other two it was the left side. All patients were seated comfortably in an arm chair in a dimly lit room with their eyes open looking straight at a defined spot on the level of their eyes. Their forearms were supported on and their hands hanging freely from the armrests. Surface EMG was recorded from the forearm extensors and flexors on the more affected side with two silver-chloride electrodes positioned close to the motor points of both muscles. EEG was recorded in parallel with a standard 64-channel recording system (Neuroscan, Herndon, VA, USA) using a linked mastoid reference. A standard EEG cap was used with electrode positions according to the extended 10–20 system. EEG and EMG were band pass filtered (EMG 30–200 Hz; EEG 0.05–200 Hz) and digitized with a sampling rate of 1000 Hz. The digitized data were stored in a computer and analysed off-line. Individual recordings were of 1–3 min duration. The number of recordings performed in each patient varied between 2 and 3 depending on the comfort of the subject.

EMG was full-wave rectified and the EEG was made reference free by Hjorth transformation (Hjorth, 1975). The combination of band pass filtering and rectification is the common demodulation procedure for tremor EMG (Journee, 1983). Only 49 EEG electrodes were used. The boundary electrodes were used only for the Hjorth transformation and not for the subsequent analysis. Each record was segmented into a number of 1-s-long high-quality epochs discarding all those data sections with visible artefacts. For each record, depending on the length of the recording and the quality of the data, between 40 and 240 segments of 1s were used for the analysis.

2.2. Data analysis

2.2.1. Coherence and phase

Coherence reveals components that are common to two signals in the frequency domain. Let the two concurrently recorded signals be $x(t)$ and $y(t)$ of length N. The arithmetic mean is set to zero and the standard deviation is set to one for both data sets. The data sets of length N were divided into M disjoint segments of length L, so that $N = LM$. Power spectra $S_{xx}(\omega)$ and $S_{yy}(\omega)$ of the signals x and y are computed as the Fourier transform of the autocorrelation function in each window. The cross spectrum $S_{xy}(\omega)$ is the Fourier transform of the crosscorrelation function of the signal x and y in each window. The power spectra and the cross spectrum are averaged across all the segments to get the estimate of the same. To this end coherence is obtained as follows:

$$\widehat{C}(\omega) = \frac{\left|\widehat{S}_{xy}(\omega)\right|^2}{\widehat{S}_{xx}(\omega)\widehat{S}_{yy}(\omega)} \tag{1}$$

The overcap indicates the estimate of that quantity (Halliday et al., 1995).

The coherence measures the linear time-invariant (LTI) relationship between the two signals $x(t)$ and $y(t)$. The confidence limit which indicates the significance of the coherence at a particular frequency is calculated at the 100%α as given by $1-(1-\alpha)^{1/(M-1)}$ (Halliday et al., 1995; Govindan et al., 2005) where α is set to 0.99, so the confidence limit is $1-0.01^{1/(M-1)}$. The value of coherence (see Fig. 1(A))

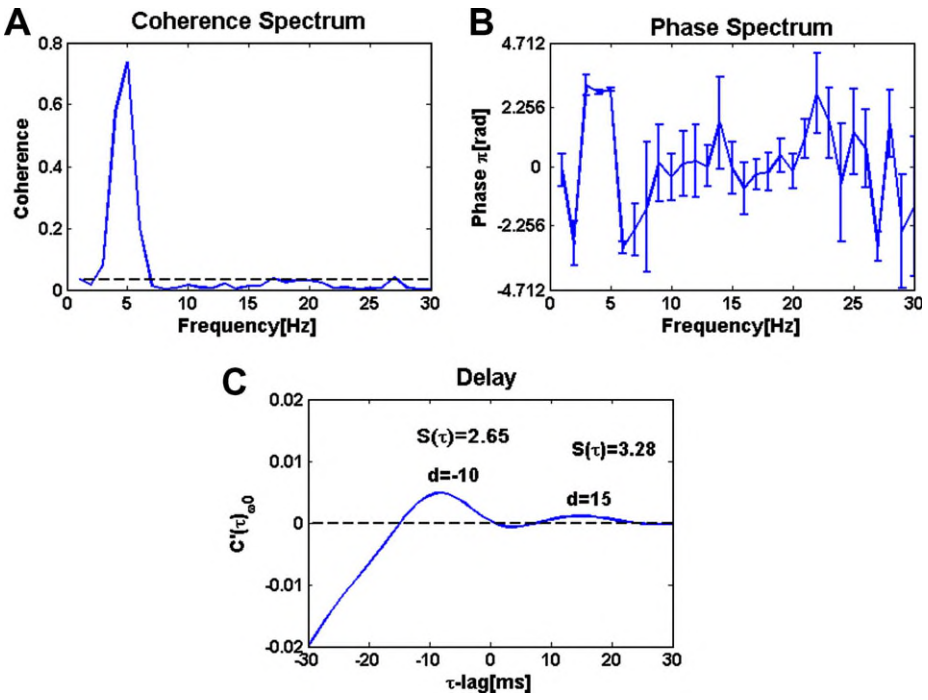

Fig. 1. Representative example of a corticomuscular (EEG–EMG) coherence spectrum (A), phase spectrum (B) and coherence as a function of time shift (C) for one recording in a Parkinsonian tremor patient. The narrow band coherence around the tremor frequency of 5 Hz is displayed in (A), the phase shift between EEG and EMG at this coherent frequency is close to π as displayed in (B). The maxima in the maximising coherence analysis (C) are at 15 and 10 ms.

above this confidence limit is considered to indicate correlation between the two time series and the values below this confidence limit indicate the absence of correlation between the two time series. The length L should be chosen optimally in order to have a good compromise between sensitivity and reliability (Govindan et al., 2005). In all our analyses a fixed segment length of $L = 1000$ (1 s) is used.

The phase spectrum $\hat{\phi}(\omega)$ (see Fig. 1(B)) which is the argument of the cross spectrum (Halliday et al., 1995; Muller et al., 2003) and its upper and lower 95% confidence interval are given by

$$\hat{\phi}(\omega) = \arg\left\{\widehat{S}_{xy}(\omega)\right\} \tag{2}$$

$$\hat{\phi}(\omega) \pm 1.96\left[\frac{1}{2M}\left(\frac{1}{\widehat{C}(\omega)} - 1\right)\right]^{\frac{1}{2}} \tag{3}$$

The time delay can be estimated in the frequency domain, by fitting a straight line to the phase spectrum in the frequency band of significant coherence as given in Eq. (4)

$$\hat{\phi}(\omega) = \omega\delta + c, \tag{4}$$

where δ is the slope of the line which is the time delay and c is the phase shift. This method is suitable only for broad band coherent signals and lacks the ability to resolve the time delay from narrow band coherent signals which are often observed in the biological data (see Fig. 1(A)).

2.2.2. Delay estimation for narrow band coherent signals

The delay δ between two narrow band coherent time series $x(t)$ and $y(t)$ is estimated by maximising the coherence. Due to a time delay there will be a time misalignment between the two time series, thereby causing a reduction in coherence estimated between them. In order to compensate for this reduction in coherence, we shift one of the time series say $x(t)$ by a time lag(τ) keeping $y(t)$ constant and estimating the coherence $C(\tau)_{\omega_0}$ in a particular frequency band as a function of τ. At $\tau = \delta$ the value of $C(\tau)_{\omega_0}$ will reach a maximum. This process is repeated for the other time series $y(t)$ to estimate the time delay, if any, in the other direction. Due to shifting one time series by a time lag τ, the length of the shifted time series will be less than the unshifted time series by $N - \tau$ data points. The extra data points in the unshifted time series are discarded, in order to have the same length for both time series. Because, coherence is a relative measure and changes with the length of the data, the points corresponding to the maximum lag are discarded from the total length of the data. Finally, we consider only the length of the data which is an integer multiple of L. Due to this the coherence $C(\tau)_{\omega_0}$ estimated in all lags will have the same confidence limit. This verifies that the maximum value in coherence is obtained due to the time delay and not because of the difference in lengths of data (Govindan et al., 2005).

The significance of the delay τ is checked by the confidence limit, but to get the variability in the estimated delay, we adapt surrogate analysis. The error bars for the estimated delay are calculated using the surrogate analysis. The surrogates are generated by utilising one of the basic assumptions of spectral analysis, that disjoint data segments of a time series are independent. We shuffle the disjoint data segments of one of the time series randomly, this is performed for only

the time series from which the time delayed information is assumed to flow to the other time series. In this type of surrogate the cross spectrum is different but the original spectrum of both the time series is unchanged. We estimate 19 different surrogates for all the analysis and determine the time delay coherence function $C(\tau)_{\omega_0}^{\text{surr}}$ for all the realisations. We make a null hypothesis that coherence calculated between the two time series is obtained due to spurious correlations (Theiler et al., 1992). The $S(\tau)$ is the significance of difference between $C(\tau)_{\omega_0}$ and $C(\tau)_{\omega_0}^{\text{surr}}$ as

$$S(\tau) = \left| C(\tau)_{\omega_0} - \left\langle C(\tau)_{\omega_0}^{\text{surr}} \right\rangle \right| \Big/ \sigma\left[C(\tau)_{\omega_0}^{\text{surr}} \right] \tag{5}$$

where $\langle . \rangle$ indicates the average over different realisations of surrogates and $\sigma[.]$ indicates the standard deviation between different realisations. If $S(\tau) > 2$ the null hypothesis is rejected and $C(\tau)_{\omega_0}$ is used in further analysis, otherwise the values are not considered for further analysis. The error bars are calculated by subtracting $C(\tau)_{\omega_0}^{\text{surr}}$ from $C(\tau)_{\omega_0}$ and determine the delay for every surrogate subtracted realisation. The mean values of these delays are given as the delay between the two time series $x(t)$ and $y(t)$ and the standard deviation is taken as the error bar. In order to have clarity of the delay, we plot in Fig. 1(C) $C'(\tau)_{\omega_0}$, in which the value of coherence $C(\omega_0)$ is at $\tau = 0$ and the average of all surrogates at $\tau = 0$ is given by $\langle C(\omega_0)^{\text{surr}} \rangle$. Thus $C'(\tau)_{\omega_0}$ will pass through a zero value at $\tau = 0$ and will attain maximum at $\tau = \delta$ (Govindan et al., 2005).

$$C'(\tau)_{\omega_0} = [C(\tau)_{\omega_0} - \langle C(\tau)_{\omega_0}^{\text{surr}} \rangle] - [C(\omega_0) - \langle C(\omega_0)^{\text{surr}} \rangle] \tag{6}$$

We estimate the delay between the two time series as

$$\delta = \arg\max_{\tau} C'(\tau)_{\omega_0} \tag{7}$$

In all of our analyses for the model system and also for the biological system, we have used a frequency resolution of 1 Hz. The average delay of the system is calculated by weighting the delay obtained for each electrode (when it is qualified in the surrogate analysis) by a fraction of the coherence $C(\omega_0)$ value that each electrode contributes to the whole system. We define the fraction of the coherence values as the ratio of the coherence value of the respective electrode to the sum of the coherences of all coherent EEG electrodes in the contralateral central region (for details we refer to Govindan et al., 2005). By doing so, electrodes showing higher tremor-related correlations will contribute more to the delay of the system.

3. Results

3.1. Application to model system

In this section, the method of maximising coherence is applied to coupled second order autoregressive AR(2) process. The way of modelling delayed signals using low-order autoregressive model (which delivers a specific rhythm with a noise), and then introducing timeshifts of this signal with simultaneous addition of another noise component is frequently used to mimic biomedical signals (Lindemann et al., 2001). The AR2 process is defined as:

$$y_0(t) = a_1 y_0(t-1) + a_2 y_0(t-2) + \eta_0(t) \tag{8}$$

where a_1 and a_2 are the AR2 coefficients which are evaluated as

$$a_1 = 2\cos(2\pi/T)\exp(-1/\tau) \tag{9}$$

$$a_2 = -\exp(-2/\tau) \tag{10}$$

In Eq. (8) $\eta_0(t)$ is a Gaussian white noise process with zero mean and unit variance. We arbitrarily choose the sampling frequency to be 1000 Hz. In the biological situation Fig. 1(A), the coherence between the two time series is narrow band of 5 Hz. In order to model this in the system we used a band pass filtered version of the AR2 process which was then delayed by 10 ms (10 sampling units). The band pass filtering was done using 4th order butterworth filter within narrow frequency band of 4 and 6 Hz.

The phase shift was introduced to the model system and then the delay was measured using the maximising coherence method. For a given time series x, the phase shift was introduced by calculating the Fourier transform $F(\omega)$ of the time series. The complex-valued $F(\omega)$ is divided into amplitude signal $a(\omega)$ and phase signal $\psi(\omega)$. These are further divided into $a_{\text{P}}(\omega), a_{\text{N}}(\omega)$ and $\psi_{\text{P}}(\omega), \psi_{\text{N}}(\omega)$ for positive (P) and negative (N) frequencies. The desired phase shift c is added to $\psi_{\text{P}}(\omega)$ and the modified $\psi'(\omega) = (\psi_{\text{P}}(\omega) + c)$ is multiplied with $a_{\text{P}}(\omega)$ to get the phase-shifted signal as follows:

$$F'_{\text{P}}(\omega) = a_{\text{P}}(\omega) \cdot \mathrm{e}^{\mathrm{i}\psi'_{\text{P}}(\omega)} \tag{11}$$

where $F'_{\text{P}}(\omega)$ is the positive frequency part of the modified (complex-valued) signal. The negative part $F'_{\text{N}}(\omega)$ is obtained by taking the complex conjugate of the positive part (i.e.) $F'_p(\omega)^{\dagger}$ where † indicates complex conjugate operator. Finally inverse Fourier transform is applied to $F'(\omega)$ to get the phase-shifted signal in time domain.

In order to test the method of maximising coherence in the model system, we introduced different amounts of phase shifts (0–2π) to the system with a standard delay of 10 ms. The different phase shifts only lead to a small degree of uncertainity, but the estimated delay never reflected the time equivalent of the phase-shift. For example for the 5-Hz process discussed in Fig. 1, a phase-shift of π is equivalent to 100 ms. Thus if we had used Eq. (2) to measure the delay we would have wrongly estimated it at around 100 ms. But the method of maximising coherence for delay estimation is able to correctly capture the delay around 10 ms (see Fig. 2) by separating phase-shift and delay in narrow band coherent signals.

3.2. Application to Parkinsonian tremor

3.2.1. Intermuscular phase-shift and delay

All of our patients showed phase-shifts between forearm extensors and flexors of around π radians indicating a reci-

procal alternating pattern of activation Fig. 3(A). The delay analysis between both muscles given in Fig. 3(B) shows values very close to zero indicating that there was no relevant delay between the extensor and flexor even though their bursts were clearly out of phase.

3.2.2. Corticomuscular phase-shift and delay

In accordance with previous studies all the coherent EEG electrodes were located in central region contralateral to the respective muscle (Fig. 4, Hellwig et al., 2000). An example of a corticomuscular coherence, phase spectrum and delay analysis between the forearm extensor muscle and an EEG electrode on the hemisphere contralateral to this muscle is given in Fig. 1. The narrow band coherence at 5 Hz can be clearly seen. The phase-shift between the cortex and the muscle signal is around π radians. The time equivalent of this phase shift in a 5-Hz oscillation would be around 100 ms. The delay estimation shows, however, that there is a delay of only 15 ms from EEG to EMG and 10 ms from EMG to EEG. This discrepancy between the time equivalent of the phase shift and the delay already indicates that there is a combination of a constant phase and a delay in the corticomuscular interaction.

The corticomuscular phase shifts for all coherent contralateral cortical electrodes and recordings and the flexor and extensor muscles are given in Fig. 5. The phase-shift values for flexor and extensor muscles from the same recordings are connected by a line. The corticomuscular phase shifts are very variable but the connecting lines illustrate that the phase shifts have opposite signs for flexors and extensors and that the difference between the corticomuscular phase shifts to the antagonistic muscles is between $3\pi/4$ and π for all EEG electrodes and all recordings.

Conversely, in case of the corticomuscular delays estimated for different electrodes and flexors and extensors separately (see Fig. 6) the connecting lines between flexors and extensors are relatively straight indicating that the EEG–EMG (positive values) and EMG- EEG (negative values) delays were very similar for flexors and extensors (differences mainly between 0 and 5 ms). The average corticomuscular delays taking into account all the coherent cortical electrodes (see Section 2) are given as round open dots for each recording. The error bar for each of these average delays is given as standard deviations next to the round open dots in the figure. Average delays range mainly between 10 and 25 ms in both directions and are again well comparable between the antagonistic muscles (mean delays $\pm$ std:. Ext. right-Cortex: 15.58 ± 7.21, Flex. right-Cortex: 17.02 ± 7.02, Cortex-Ext. right: 15.69 ± 2.12, Cortex-Flex. right: 12.89 ± 4.68, Ext. left-Cortex: 15.83 ± 3.81, Flex. left-Cortex: 18.1 ± 4.90, Cortex-Ext. left: 14.02 ± 4.15, Cortex-Flex. left: 17.26 ± 6.24) In the majority of recordings there was a bidirectional delay with one dot at positive and one at negative values. For some of the electrodes and some recordings there also were unidirectional delays. It is of note that these delays and the vast majority of the bidirectional delays were clearly different from zero. In a minority of recordings we did not find any significant delays that passed the surrogate analysis (see Section 2).

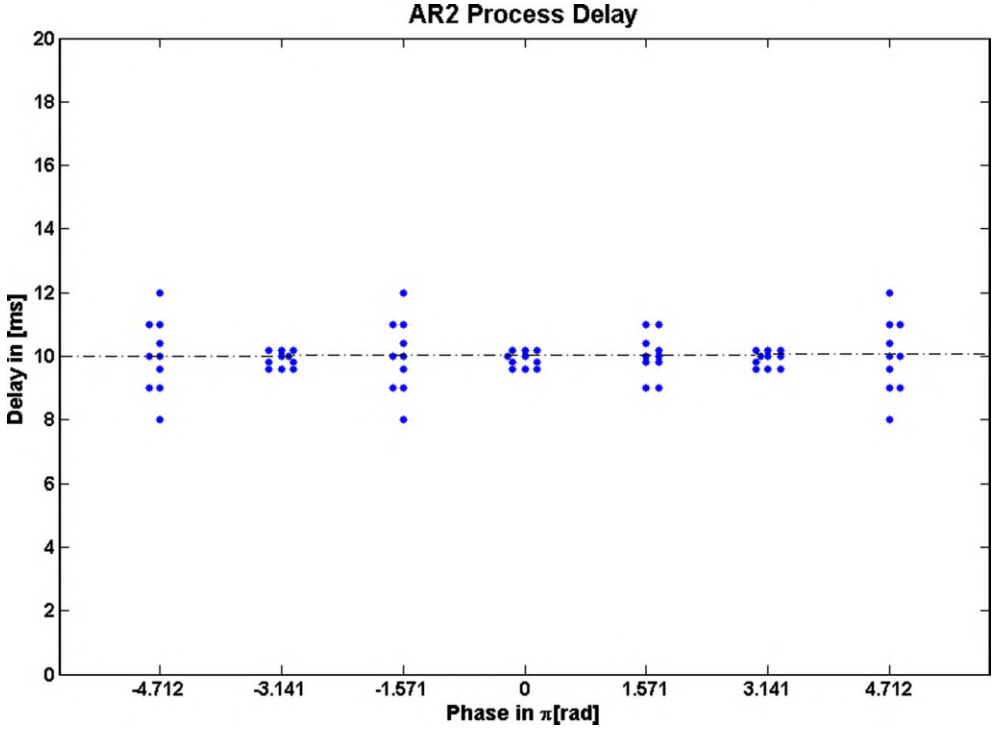

Fig. 2. Delay estimation between a narrow band pass filtered AR2 process and its delayed (10 ms) copy for different phase shifts. It is clear that the estimated delay is very close to the real delay of 10 ms independent of the phase shift. Thus the phase shift only marginally influenced the delay estimation.

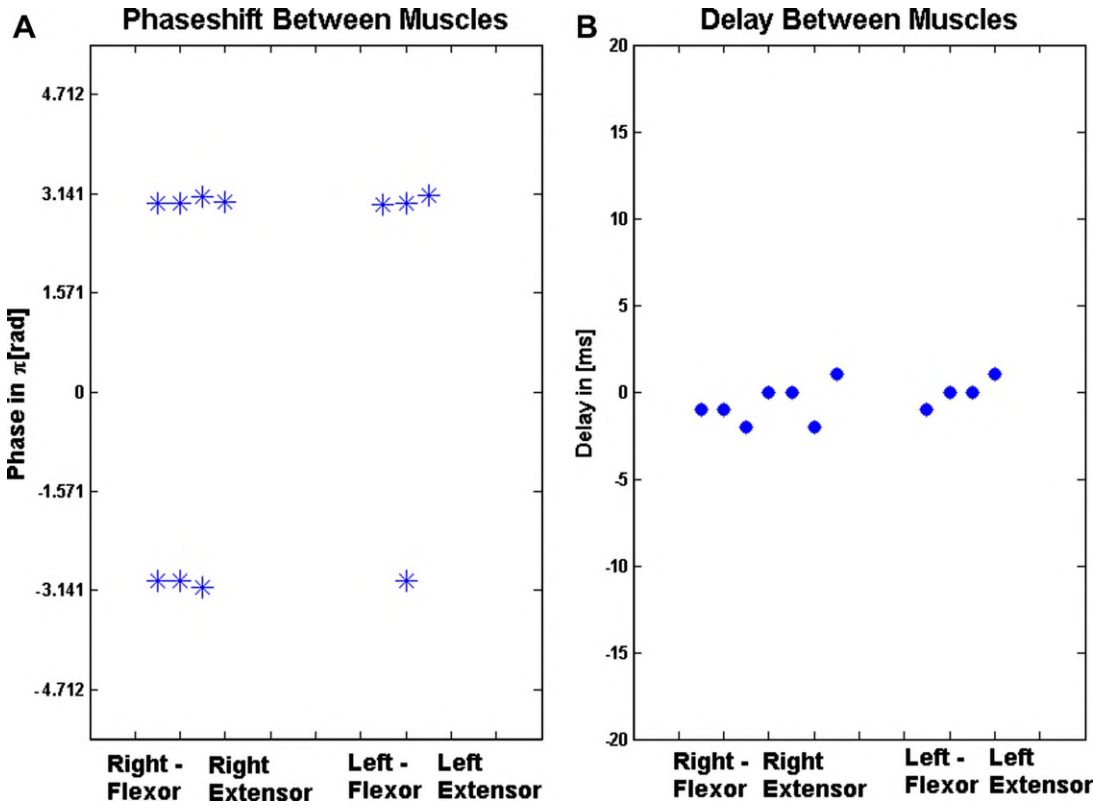

Fig. 3. Phase shifts (A) and delays (B) between antagonistic forearm muscles on in Parkinsonian tremor. As expected the phase shift between these muscles was close to π or $-\pi$ indicating a reciprocal alternating pattern (A). Conversely the corresponding delays (B) between the two muscles were all very close to zero indicating that there was hardly any delay between them.

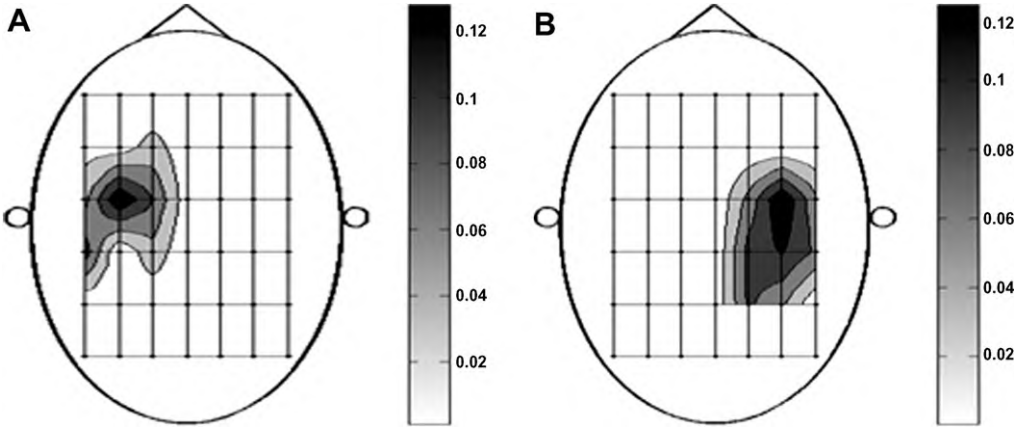

Fig. 4. Two representative isocoherence maps from two recordings of two different patients. The coherence above the significance level is gray scale coded according to the bars on the right side. (A) displays the cortical area that was coherent with a right sided rest tremor and (B) shows this with respect to a left sided tremor in another patient. In both cases the coherent area is clearly restricted to the contralateral cortex and is centered around the central region.

4. Discussion

The application of the new delay analysis in conjunction with the phase spectra in the model system confirms that the combination of these methods can distinguish between constant phase shift and delay.

In the application to the situation in Parkinsonian tremor it proves to be capable of dissecting the interactions within a narrow band oscillating system. The timing between the tremor bursts in antagonistic muscles is a pure phase shift without any delay between them. Thus the reciprocal alternating pattern between antagonistic muscles often encountered in Parkinsonian tremor is generated as a fixed pattern, similar to the pattern generation in voluntary rhythmic hand movements or gait. This is not surprising as the shift between the tremor bursts in antagonistic

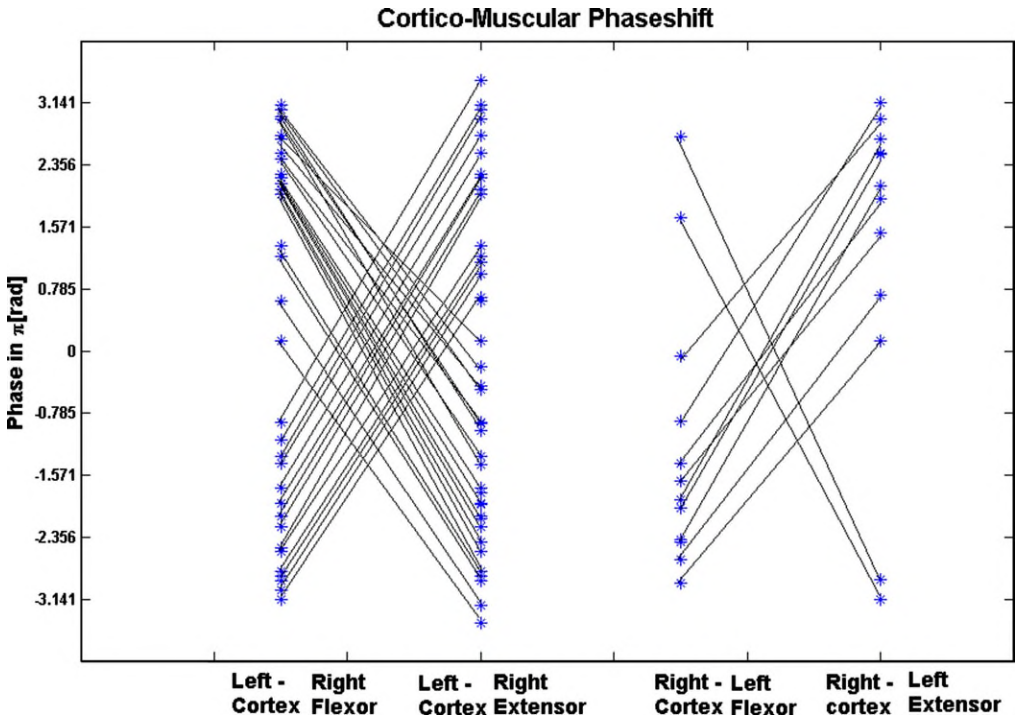

Fig. 5. Phase shifts between the trembling forearm extensor and flexor muscles and the coherent EEG electrodes over the contralateral hemisphere. Phase shifts for the same EEG electrodes and recordings were connected by a line. These connecting lines illustrate that the corticomuscular phase shift is reversed between flexor and extensor muscles and reaches values close to π and $-\pi$. This is in line with the reciprocal alternating activity of the two muscles.

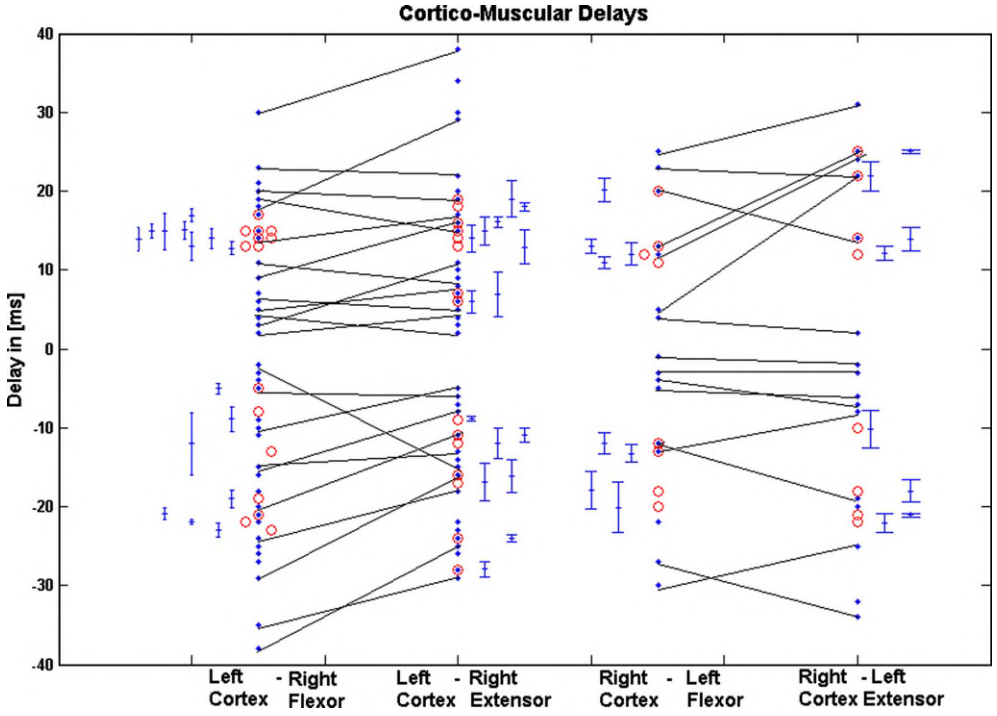

Fig. 6. Corticomuscular delays between the forearm extensor and flexor muscles and the EEG electrodes over the contralateral hemisphere. Positive values on the ordinate indicate EEG–EMG whereas negative values indicate EMG-EEG delays. Delays for the same EEG electrodes and recordings are connected by a line. The average delays for all EEG electrodes of one recording are given by the round open dots. The error bars of these average delays are given by their standard deviations next to each of these dots. In contrast to the phase shifts the delays were similar for both muscles with the mean delays being exactly in the same range.

muscles has always been viewed as a 'phase shift' (Spieker et al., 1995; Deuschl et al., 2000; Milanov, 2001). Our data confirm this quantitatively for the first time.

The pure phase shift between the antagonistic muscles in the periphery will inevitably have an influence on the corticomuscular phase relationship as the phase shift between cortex and extensor and cortex and flexor should reflect the intermuscular phase shift to some extent. Indeed, we found opposite signs and a difference of $3\pi/4$ between the corticomuscular phase shifts to the flexor and extensor muscles on the same side. This marked difference clearly indicates that the time equivalents of the corticomuscular phase shifts hardly reflect the delays but are dominated by other factors, e.g. the peripheral pattern of tremor bursts. Nevertheless, the maximising coherence method enabled us to independently estimate the corticomuscular delays indicating a transmission from cortex to muscle and feedback to the cortex at the tremor frequency. This is in line with previous studies (Volkmann et al., 1996; Timmermann et al., 2003) which have, however, concentrated on the interaction between cortex and one of the antagonistic forearm muscles only. Our comparison between both muscles shows that in contrast to the phase shifts the delays were almost identical for the flexor and extensor muscles, differing by less than 5 ms in most recordings. Given the close vicinity of the two muscles this is plausible, and the delay times in the range of 10–25 ms would be in keeping with fast corticospinal transmission (Rothwell et al., 1991) to and feedback of the tremor activity from both muscles.

The vast majority of the corticomuscular and musculocortical delays even for single electrodes were clearly different from zero whereas the EMG–EMG delays were reproducibly very close to zero. This confirms that the maximising coherence method is able to distinguish between zero and non-zero delays also in case of bidirectional interactions.

Taking our results for the intermuscular and corticomuscular interaction in Parkinsonian tremor together they indicate that there is a fixed activation pattern determining the relationship between antagonistic muscle bursts and on the other hand there is a cortical correlate that is transmitted to both of these muscles with similar delays. However, our results do not reveal at which level of the CNS these two mechanisms interact. Spinal interneuronal system would certainly be able to produce such a reciprocal alternating pattern (Rossignol and Dubuc, 1994), on the other hand there are good hints that such timing relationships between different muscles could already be implemented on the motor cortical level (Rathelot and Strick, 2006), and subcortical/brainstem centers which are very likely part of the generating network for Parkinsonian tremor (Deuschl et al., 2000; Lang and Zadikoff, 2005) may equally be involved.

Nevertheless, our data clearly show that delay and phase shift should be separated carefully when trying to characterize the mode of interaction also in narrow band oscillating systems. The method of maximising coherence (Gross et al., 2000; Govindan et al., 2005, 2006) can obviously estimate the delay between two coupled narrow band signals independently of additional phase shifts between the signals. In view of our results all approaches attempting to use phase-shift measures as a basis for delay estimation in narrow-band signals (Hellwig et al., 2000; Gross et al., 2000; Timmermann et al., 2003) seem problematic.

Acknowledgement

This work was supported by the German Research Council (Deutsche Forschungsgemeinschaft Grant RA 1005/1-1).

References

Boose A, Spieker S, Jentgens C, Dichgans J. Wrist tremor: investigation of agonist–antagonist interaction by means of long-term EMG recording and cross-spectral analysis. Electroencephalogr Clin Neurophysiol 1996;101(4):355–63.

Brown P. Cortical drives to human muscle: the Piper and related rhythms. Prog Neurobiol 2000;60(1):97–108.

Deuschl G, Bain P, Brin M. Consensus statement of the movement disorder society on tremor, Ad Hoc Scientific Committee. Mov Disord 1998;13(Suppl. 3):2–23.

Deuschl G, Raethjen J, Baron R, Lindemann M, Wilms H, Krack P. The pathophysiology of Parkinsonian tremor: a review. J Neurol 2000;247(Suppl. 5):V33–48.

Govindan RB, Raethjen J, Kopper F, Claussen JC, Deuschl G. Estimation of delay time by coherence analysis. Physica A 2005;350:277–95.

Govindan RB, Raethjen J, Arning K, Kopper F, Deuschl G. Time delay and partial coherence analyses to identify cortical connectivities. Biol Cybern 2006;94(4):262–75.

Grillner S. Control of locomotion in bipeds tetrapods and fish. In: Brooks VB, editor. Handbook of physiology. Bethesda, ML: American Physiological Society; 1981.

Grillner S. Biological pattern generation: the cellular and computational logic of networks in motion. Neuron 2006;52(5):751–66.

Gross J, Tass PA, Salenius S, Hari R, Freund HJ, Schnitzler A. Cortico-muscular synchronization during isometric muscle contraction in humans as revealed by magnetoencephalography. J Physiol 2000;527(Pt. 3):623–31.

Halliday DM, Rosenberg JR, Amjad AM, Breeze P, Conway BA, Farmer SF. A frame work for the analysis of mixed time series /point process data-theory and application to study of physiological tremor, single motor unit discharges and electromyograms. Prog Biophys Mol Bio 1995;64:237–8.

Hellwig B, Haussler S, Lauk M, Guschlbauer B, Koster B, Kristeva-Feige R. Tremor correlated cortical activity detected by electroencephalography. Clin Neurophysiol 2000;111(5):806–9.

Hjorth B. An on-line transformation of EEG scalp potentials into orthogonal source derivations. Electroencephalogr Clin Neurophysiol 1975;39(5):526–30.

Hughes AJ, Daniel SE, Kilford L, Lees AJ. Accuracy of clinical diagnosis of idiopathic Parkinson's disease: a clinico-pathological study of 100 cases. J Neurol Neurosurg Psychiatry 1992;55(3):181–4.

Journee HL. Demodulation of amplitude modulated noise: a mathematical evaluation of a demodulator for pathological tremor EMG's. IEEE Trans Biomed Eng 1983;30(5):304–8.

Kay BA, Saltzman EL, Kelso JA. Steady-state and perturbed rhythmical movements: a dynamical analysis. J Exp Psychol Hum Percept Perform 1991;17(1):183–97.

Lang AE, Zadikoff C. Parkinsonian tremor. In: Lyons KE, Pahwa R, editors. Handbook of essential tremor and other tremor disorders. Boca Raton: Taylor and Francis; 2005. p. 195–220.

Lindemann M, Raethjen J, Timmer J, Deuschl G, Pfister G. Delay estimation for cortico-peripheral relations. J Neurosci Methods 2001;111(2):127–39.

Milanov I. Electromyographic differentiation of tremors. Clin Neurophysiol 2001;112(9):1626–32.

Mima T, Hallett M. Electroencephalographic analysis of cortico-muscular coherence: reference effect, volume conduction and generator mechanism. Clin Neurophysiol 1999;110(11):1892–9.

Muller T, Lauk M, Reinhard M, Hetzel A, Lucking CH, Timmer J. Estimation of delay times in biological systems. Ann Biomed Eng 2003;31(11):1423–39.

Rathelot JA, Strick PL. Muscle representation in the macaque motor cortex: an anatomical perspective. Proc Natl Acad Sci USA 2006;103(21):8257–62.

Rossignol S, Dubuc R. Spinal pattern generation. Curr Opin Neurobiol 1994;4(6):894–902.

Rothwell JC, Thompson PD, Day BL, Boyd S, Marsden CD. Stimulation of the human motor cortex through the scalp. Exp Physiol 1991;76(2):159–200.

Spieker S, Boose A, Jentgens C, Dichgans J. Long-term tremor recordings in parkinsonian and essential tremor. J Neural Transm Suppl 1995;46:339–49.

Theiler J, Longtin A, Galdrikan B, Farmer JD. Testing for nonlinearity in time series. The method of surrogate data. Physica D 1992;58:77–94.

Timmermann L, Gross J, Dirks M, Volkmann J, Freund HJ, Schnitzler A. The cerebral oscillatory network of parkinsonian resting tremor. Brain 2003;126(Pt 1):199–212.

Volkmann J, Joliot M, Mogilner A, Ioannides AA, Lado F, Fazzini E. Central motor loop oscillations in parkinsonian resting tremor revealed by magnetoencephalography. Neurology 1996;46(5): 1359–70.